

RESEARCH REPORT

New alleles of the wheat domestication gene *Q* reveal multiple roles in growth and reproductive development

Julian R. Greenwood^{1,2}, E. Jean Finnegan¹, Nobuyoshi Watanabe³, Ben Trevaskis¹ and Steve M. Swain^{1,*}

ABSTRACT

The advantages of free threshing in wheat led to the selection of the domesticated *Q* allele, which is now present in almost all modern wheat varieties. *Q* and the pre-domestication allele, *q*, encode an AP2 transcription factor, with the domesticated allele conferring a free-threshing character and a subcompact (i.e. partially compact) inflorescence (spike). We demonstrate that mutations in the miR172 binding site of the *Q* gene are sufficient to increase transcript levels via a reduction in miRNA-dependent degradation, consistent with the conclusion that a single nucleotide polymorphism in the miRNA binding site of *Q* relative to *q* was essential in defining the modern *Q* allele. We describe novel gain- and loss-of-function alleles of *Q* and use these to define new roles for this gene in spike development. *Q* is required for the suppression of ‘sham ramification’, and increased *Q* expression can lead to the formation of ectopic florets and spikelets (specialized inflorescence branches that bear florets and grains), resulting in a deviation from the canonical spike and spikelet structures of domesticated wheat.

KEY WORDS: Wheat, Spike, Inflorescence, AP2, Domestication, microRNA

INTRODUCTION

The causal molecular mechanism for the domestication of *Q* is thought to be an amino acid change in the predicted *Q* protein (Simons et al., 2006) and/or a single nucleotide polymorphism (SNP) present in a presumed miRNA binding site of *Q* (Sormacheva et al., 2015; Chuck et al., 2007). Unlike the domesticated homeoallele *Q* (chromosome 5A) (Faris et al., 2003), the B and D homeoalleles of hexaploid bread wheat are thought to be a pseudogene and expressed at a low level, respectively (Zhang et al., 2011). *Q* is a member of the AP2 class of transcription factors, which are known to influence many traits associated with floral transition, including both flowering time and the definition of floral organs (Aukerman and Sakai, 2003; Chuck et al., 2007; Lauter et al., 2005; Lee and An, 2012; Lee et al., 2007; Brown and Bregitzer, 2011; Varkonyi-Gasic et al., 2012). Generally, gain-of-function mutations and overexpression of *AP2* genes result in delayed flowering (Mlotshwa et al., 2006; Aukerman and Sakai, 2003; Schmid et al., 2003; Jung et al., 2007) and additional florets in the *Tasselseed6* mutant of corn (Chuck et al., 2007). Loss-of-

function mutations and reduced expression can cause early flowering and disruptions in floral patterning and determinacy (Chuck et al., 1998, 2008; Lee and An, 2012; Mlotshwa et al., 2006; Jung et al., 2007; Mathieu et al., 2009); these effects can be masked by redundant function of other *AP2* genes (Yant et al., 2010). *AP2* genes can be regulated by miR172, and mutations affecting the expression of miR172 or SNPs in either *miR172* or in its conserved target site in *AP2* genes can lead to misregulation, with the potential to increase or reduce regulatory targeting by the miRNA (Aukerman and Sakai, 2003; Chuck et al., 2007; Varkonyi-Gasic et al., 2012; Zhu et al., 2009).

RESULTS AND DISCUSSION

A dwarf, compact spike mutant was identified in an *M*₂ mutant population derived from the Australian wheat cultivar Sunstate (SS) and backcrossed to the progenitor line SS. The *F*₂ progeny of this cross could be separated into three distinct height classes, namely SS-like, intermediate (heterozygous) and short (homozygous mutant) (Fig. 1A,B), which were subsequently confirmed by genetic analysis (see below). Differences in height were substantial (Fig. 1B,C) and unambiguously separated plants into the three classes. Both heterozygous and homozygous mutant plants were characterized by a reduction in internode length relative to SS-like siblings, resulting in spike compaction and reduced overall height (Fig. 1C,D; Fig. S1). Mutant plants were also late flowering and possessed a small increase in rachis node number (nodes along the spike that potentially bear a fertile spikelet) (Fig. 1E,F).

The compact mutant resembled transgenic wheat lines with increased copy number and expression of *Q* (Simons et al., 2006; Förster et al., 2012, 2013). The mutant (hereafter called *Q'*) contained a novel single nucleotide change in the miRNA binding site of *Q* that causes an additional mismatch when aligned to the targeting miRNA Ta-miR172 (Fig. 2A; Fig. S2). No other sequence changes were observed in the coding region. Expression of *Q*, as measured by qPCR, was higher in developing inflorescences of *Q'* plants than in their SS-like siblings (Fig. 2B,C). Modified 5' RACE detected multiple *Q* cleavage products in mRNA from SS-like plants, whereas only a single cleavage product was detected from *Q'* mRNA (Fig. 2D). The most abundant class of *Q* cleavage products matched the expected product from miRNA-directed cleavage between the tenth and eleventh nucleotides within the miRNA, whereas the single *Q'* cleavage product detected was shifted by a single base. Combined with our expression data, the reduced levels of cleavage product in *Q'* indicate that the induced mismatch to Ta-miR172 results in reduced targeted mRNA degradation, and ultimately higher *Q* protein abundance. Based on its partial genetic dominance and increased mRNA expression, *Q'* appears to be a gain-of-function allele relative to *Q*. We cannot exclude the possibility that the amino acid change (G to E) in the predicted *Q* protein resulting from the *Q'* SNP also contributes to the observed phenotypes. However, similar compact spike phenotypes have been

¹CSIRO Agriculture and Food, Black Mountain Science and Innovation Park, GPO Box 1700, Canberra, Australian Capital Territory 2601, Australia. ²Research School of Biology, Australian National University, Canberra, Australian Capital Territory 2601, Australia. ³College of Agriculture, Ibaraki University, 3-21-1 Chuo, Ami, Inashiki, Ibaraki 300-0393, Japan.

*Author for correspondence (steve.swain@csiro.au)

© S.M.S., 0000-0002-6118-745X

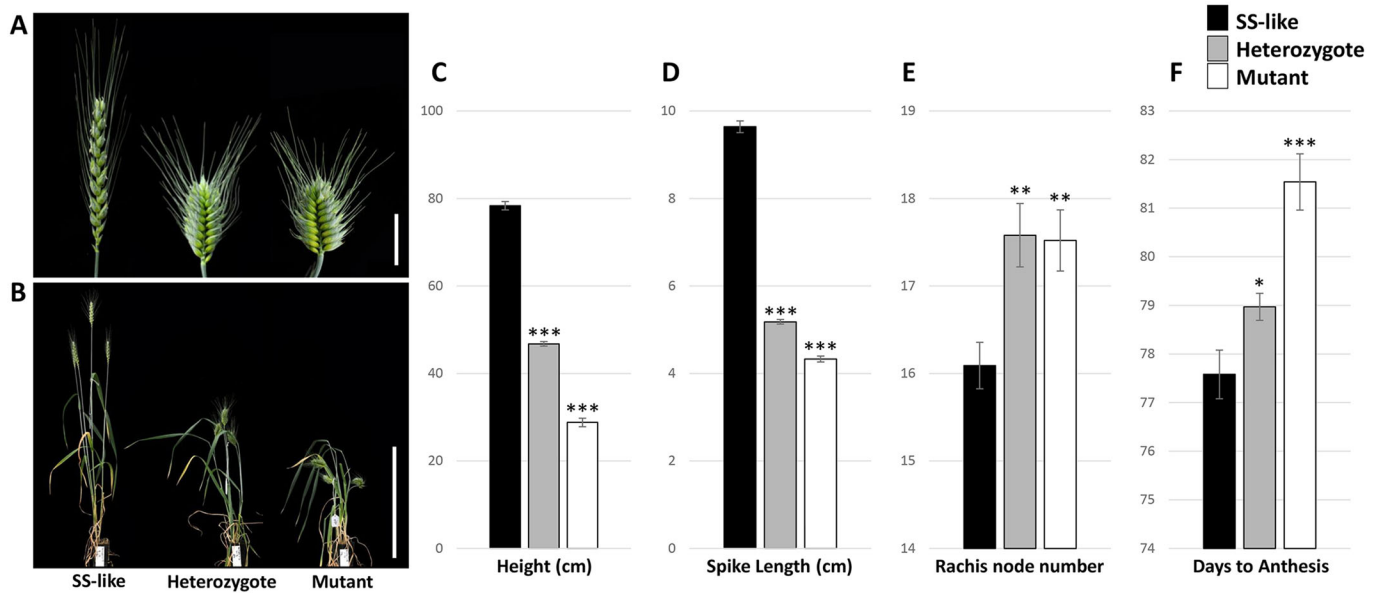


Fig. 1. Identification and characterization of a compact spike mutant. (A) Adult wheat inflorescence (spike) of the Sunstate (SS)-like sibling line, heterozygous line and homozygous mutant line. Scale bar: 3 cm. (B) SS-like, heterozygous and homozygous mutant plants at maturity. Scale bar: 30 cm. (C–F) Plant height (C), spike length (D), rachis node number (number of nodes along the spike, E) and days to anthesis (flowering time, F) of SS-like, heterozygous and compact spike mutant plants. Data are presented as mean \pm s.e.m. $n=33$ SS-like, $n=35$ heterozygous, $n=22$ mutant. * $P<0.05$, ** $P<0.01$, *** $P<0.001$, compared with SS-like plants.

reported in transgenic plants containing an miR172 binding site mimic (MIM172) and reduced levels of miR172 (Debernardi et al., 2017), suggesting that reduced miR172 cleavage in Q' is sufficient to induce the observed phenotypes. For the barley paralog *HvAP2* (2H), both synonymous and non-synonymous mutations causing mismatches to miR172 result in compact spikes, further supporting that nucleotide mismatches without amino acid changes can affect this trait (Houston et al., 2013).

To establish that the Q' mutation was causal, we first confirmed complete genetic linkage between the Q' SNP and the reduced height/compact spike phenotypes (Fig. 3B). Second, we investigated additional alleles. Two allelic dwarf mutant lines with compact spikes, ANBW5C Dwarf (5CD) and ANBW5B Dwarf (5BD) (Fig. 3A), have previously been described and mapped to chromosome 5AL (which contains Q), although the genetic basis was not determined (Kosuge et al., 2012). Sequencing revealed that both mutant lines contained SNPs within the miRNA binding site of Q , with 5CD containing the exact same mutation as Q' and 5BD (Q' -like) featuring a unique SNP in the miRNA binding site of Q (Fig. 3C; Fig. S2). The similar phenotypes of the two independent mutants support the hypothesis that the causal effect of the Q' mutation is associated with a reduction in miR172 repression rather than with the change in the encoded amino acid. Consistent with impaired regulation by miR172, all compact spike mutants showed higher expression of Q than their sibling or parent lines in both developing inflorescence and elongating peduncle internode tissue (Fig. 3G,H).

To formally confirm that the Q' mutation was causal to the observed phenotypes, we performed a second round of mutagenesis in the Q' background. Two unique revertant alleles were isolated with SNPs in the first exon of the Q' gene: Q' -Rev1, a presumed complete loss-of-function revertant with an introduced stop codon; and Q' -Rev2, a partial revertant with an amino acid change immediately before the first predicted AP2 domain (Fig. 3C). Both 'revertants' retained the Q and Q' mutations, as expected. The Q' revertants completely (Q' -Rev1) or partially (Q' -Rev2) suppressed the phenotypic changes in Q' (see below),

confirming that changes in Q are responsible for the Q' gain-of-function phenotypes.

The presence of independent gain- and loss-of-function Q alleles in a common background allows the function of Q to be analyzed with a precision not previously possible. In contrast to Q' , Q' -Rev1 plants showed a reduction in rachis node number compared with SS-like plants, demonstrating an earlier (in terms of nodes) transition from inflorescence meristem to terminal spikelet meristem (Fig. 3F). Whereas plant height was increased in Q' -Rev1 plants compared with SS-like (Q) plants, spike length did not differ significantly (Fig. 3D,E). Reduced rachis node number in Q' -Rev1 compared with Q meant that the average internode length between each spikelet was greater, resulting in reduced spikelet density, also known as a lax spike. Compared with SS-like and Q' , the lax spikes of Q' -Rev1 were difficult to hand thresh (Fig. S3), consistent with observations of plants containing pre-domestication q , or 5A deletions that lack domesticated Q (Faris et al., 2003; Simons et al., 2006; Förster et al., 2012), and with Q playing an important role in wheat domestication. Partial reversion of the Q' mutant phenotype in Q' -Rev2 was characterized by an increase in height and spike length relative to Q' , although not to the extent of SS-like plants (Fig. 3A).

Given that AP2 genes in other species have diverse roles in spikelet and floret development, we examined whether increased Q activity resulted in additional, previously undescribed changes in reproductive development. The two independent Q' mutants and Q' -like all exhibited several alterations in spikelet and floret development, although we focused on detailed analysis of the original Q' allele in the SS background. Q' plants produced fully formed floret-containing spikelets usually by the second rachis node from the base of the spike, whereas Q and Q' -Rev1 plants typically produced three or four rudimentary spikelets at the basal rachis nodes before producing fertile floret-bearing spikelets, as often occurs for modern wheat varieties (Fig. 4D; Fig. S4). Thus, increased Q activity can promote basal spikelet fertility as well as increase total rachis node number (Fig. 3F). A role for Q' in delaying conversion of the inflorescence to spikelet meristem is consistent

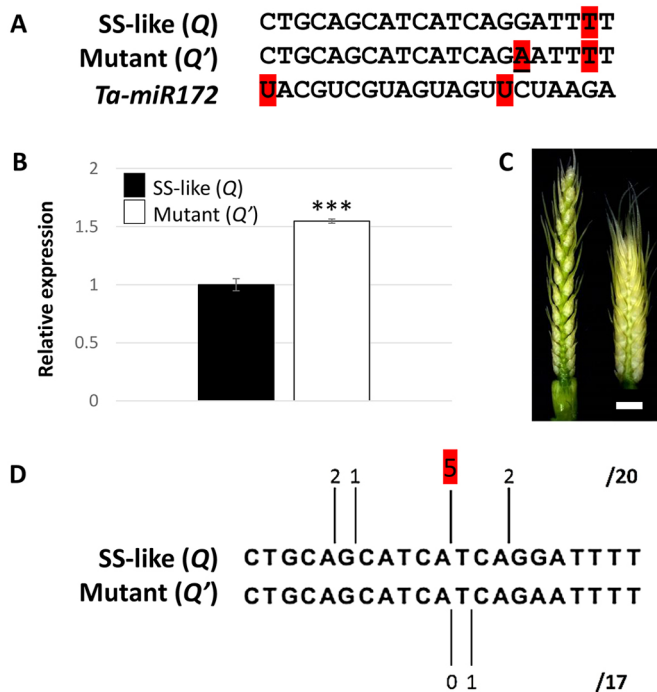


Fig. 2. The compact spike mutant *Q'* contains a novel SNP in the miRNA binding site that leads to changes in transcriptional regulation.

(A) Sequence alignment showing the miRNA binding site sequence of SS-like with the domesticated *Q* allele and the mutant (*Q'*), and the complementary wheat Ta-miR172 sequence. The miRNA mismatch underlying the domestication *Q* allele (C to T) is indicated by the 'T' highlighted in red, and is present in both *Q* and *Q'*. The 'U's highlighted in red in the miR172 sequence represent mismatches with all known *Q* sequences. The *Q'* mutation is highlighted in red and underlined. (B) Expression of *Q* in SS-like and mutant inflorescence tissue harvested at the beginning of internode elongation (~10 mm inflorescences at terminal spikelet stage). Data are presented as mean±s.e.m. of four biological replicates. ****P*<0.001. (C) Developing inflorescence of SS-like (left) and mutant (right) plants at the early internode elongation stage when the compaction phenotype first becomes apparent. Scale bar: 2 mm. (D) Cleavage products as determined by sequencing of 5' RACE products using RNA pooled from the biological samples used for the expression analysis in B. The number of clones sequenced and their detected cleavage site location are presented (expected cleavage site of *Q* is marked in red). The total number of clones presented (20 for SS-like and 17 for *Q'*) is from sequenced clones which contained *Q* transcript.

with the recently proposed role of miR172 and *AP2* genes in regulating panicle development in rice (Wang et al., 2015).

Wheat spikelets comprise two basal glumes (always sterile) followed by an indeterminate number of florets (Fig. 4A). *Q'* plants deviated from this fundamental pattern, with spikelets often possessing floret structures in place of glumes (Fig. 4B,C; Fig. S5). In the basal and apical portion of the spike, glumes were often replaced either by rudimentary florets with only a lemma and palea, or – with increasing frequency towards the terminal spikelet – complete fertile florets (Fig. 4B,C). Florets occupying typical positions in *Q'* formed normally. SEM analysis revealed floret organs forming early in spikelet development adaxial to glume-lemma organs in *Q'* (Fig. S5), with no additional lemma-like organ visible. These ectopic florets contributed to an increase in visible florets per spikelet along the spike of *Q'* plants (Fig. 4D). Spikelets in the central portion of *Q'* spikes were less likely to form florets (partial or complete) in place of glumes (Fig. 4C). In *Q'* plants there was a tendency for the glume-like structures of the spikelet to be elongated and produce lemma-like awns, with awn length

increasing along the spike from the base to the terminal spikelet (Figs S6 and S7) independently of whether floret structures were visible. Similar phenotypes were observed in MIM172 plants with increased *Q* expression (Debernardi et al., 2017). The simplest interpretation of these *Q'* phenotypes is a replacement of glumes with partially or fully developed florets, including awned lemmas. This in turn suggests that increased *Q* activity promotes ectopic floret formation during spikelet development and, remarkably, that it can alter one of the defining features of the grasses, namely two sterile glumes at the base of each spikelet.

Another characteristic of wheat spikes is that a single spikelet is usually present at each rachis node. However, in some genetic backgrounds or under appropriate environmental conditions, two spikelets can form at a single node to generate a 'paired spikelet', which might be the equivalent of a 'spikelet pair' in plants such as corn (Boden et al., 2015 and references therein). Although absent in *Q* and *Q'-Rev1* plants, *Q'* spikes contained paired spikelets, with their frequency peaking around the central rachis nodes of the spike (Figs S8 and S9).

While increased *Q* activity has multiple effects on spike, spikelet and floret development, the loss-of-function *Q'-Rev1* allele also reveals that *Q* possesses broader, previously unidentified roles (see also Debernardi et al., 2017). Unlike *Q* and *Q'*, *Q'-Rev1* plants intermittently produced spikelets with elongated rachilla internodes and many florets (also known as 'sham ramification', reminiscent of the *shr1/exg* locus on 5A (Amagai et al., 2014, 2015) (Fig. 4D,E). This trait was more severe in tillers (data not shown) than in the main spike, but the 'extra' florets in these spikelets did not produce grains. The sham ramification trait has been mapped to chromosome 5AL, in a similar position to *Q*, and has been shown to be repressed by the presence of the D genome in some backgrounds (Alieva and Aminov, 2013; Amagai et al., 2014). In the absence of a D genome, sham ramification and extra florets were observed in tetraploid wheat lines with loss-of-function alleles of *Q* and in lines overexpressing miR172 (Debernardi et al., 2017). Debernardi et al. (2017) also report extra sterile glumes in place of florets associated with *Q* loss-of-function, although we did not observe these traits in our *Q'-Rev1* line. Our observations suggest that *Q* activity must be tightly regulated, as both increases (ectopic florets in place of glumes) and decreases (sham ramification) in expression can lead to increases in floret number, similar to reports in maize *AP2* mutants (Chuck et al., 2007, 2008).

Many of the inflorescence architecture defects of *Q'* are confined to, or more severe in, certain regions of the spike. Most notably, spike compaction (Fig. S10), replacement of glumes with florets and increased awn length all become more severe in nodes closer to the terminal spikelet (Fig. 4; Figs S6 and S7). *Q* expression exhibited temporal and spatial variation during spike development (Fig. S11), with *Q'* typically more highly expressed than *Q*, and a somewhat reciprocal relationship between *Q* and miR172 expression, consistent with the results of Debernardi et al. (2017). Increased expression of *Q* in the peduncle internode and severe reduction in the size of this internode suggest that targeted degradation of *Q* by miR172 is broadly required to ensure correct elongation of internodes (stem, rachis and rachilla) in the wheat plant, demonstrating that *Q* plays an important role throughout wheat reproductive development.

In summary, using mutagenesis and a candidate gene approach we have generated a series of gain- and loss-of-function *Q* alleles that have allowed us to identify previously unknown aspects of *Q* gene function in wheat reproductive development. The presumed miRNA mismatches in the gain-of-function mutants we have isolated confirm that the common miRNA regulation of *AP2* genes

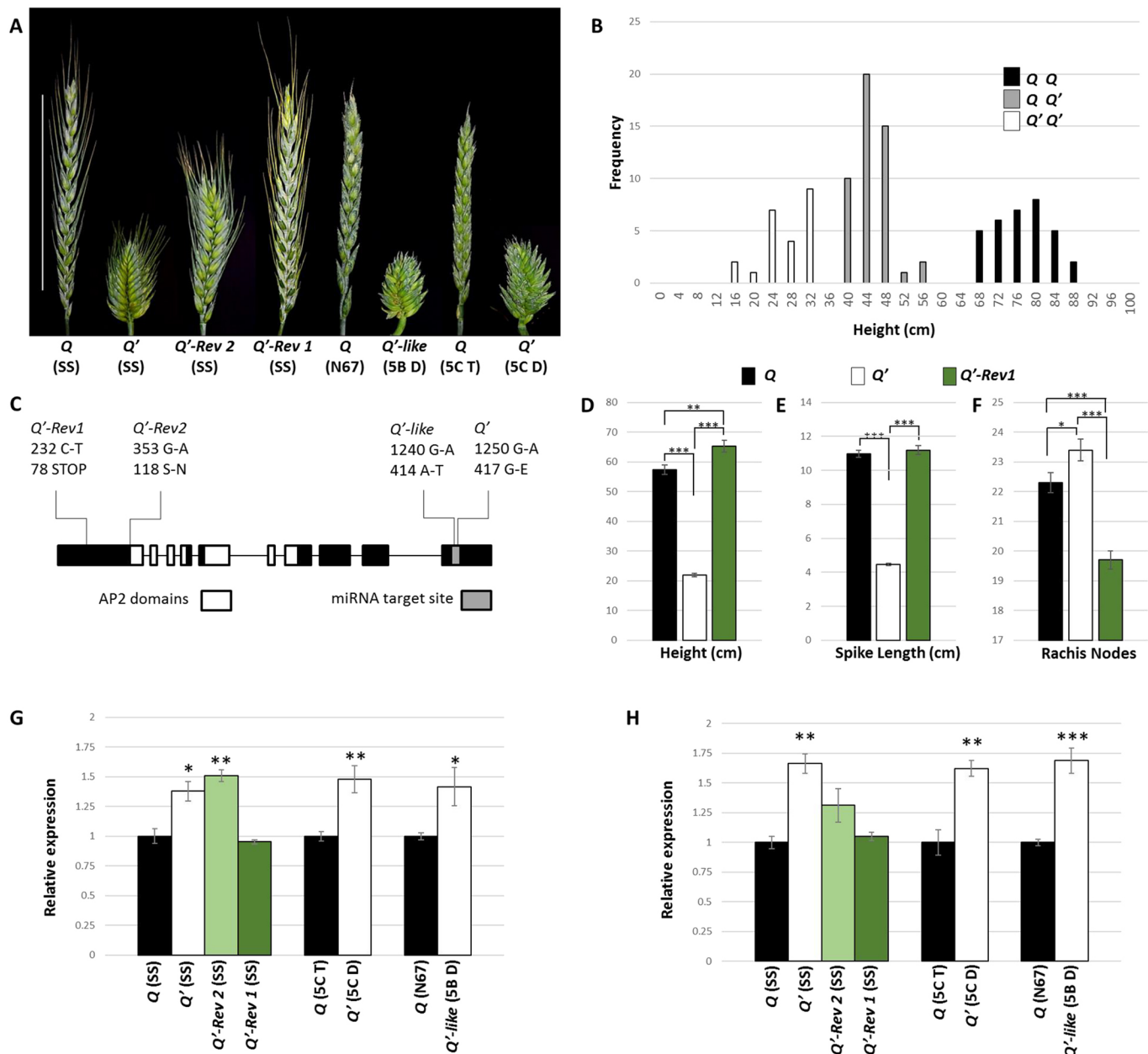


Fig. 3. Co-segregation analysis, loss-of-function mutants derived from *Q'* and additional *Q* miRNA mutants confirm that the novel SNP is causal for *Q'* phenotypes. (A) Adult wheat inflorescences of SS-like sibling (*Q*), *Q'* and secondary induced mutants *Q'-Rev2* and *Q'-Rev1* in the SS background, as well as Novosibirskaya 67 (N67) and *Q'-like* mutant ANBW5B Dwarf (5BD) in the N67 background, and sibling lines of ANBW5C Tall (5CT) and ANBW5C Dwarf (5CD, *Q'*). Scale bar: 10 cm. (B) Co-segregation of *Q* and *Q'* in the SS background showing the frequency of plants grown from heterozygous parents that fell within specific height ranges (bins covering 4 cm). Bars are shaded according to the genotype of plants within those height ranges as determined by cleaved amplified polymorphic sequence (CAPS) marker analysis. Plants segregated in agreement with a 1:2:1 ratio as determined by a chi-squared test ($P=0.281$, $n=104$ progeny). (C) *Q* gene schematic showing exons (black boxes), introns (thin lines), miRNA target site and AP2 domains. The location of *Q'* and *Q'-like* mutations and derived revertant mutations in *Q'* are shown, including nucleotide changes and predicted translational changes. (D–F) Plant height (D), spike length (E) and rachis node number (F) of *Q*, *Q'* and *Q'-Rev1* plants. Data are presented as mean \pm s.e.m. $n=10$. (G, H) Relative expression of *Q* transcript in compact mutant lines normalized to their sibling or parent line in developing inflorescences (~ 10 mm inflorescences at terminal spikelet stage) (G) and in elongating peduncle internode tissue (H). Data are presented as mean \pm s.e.m. of three biological replicates. * $P<0.05$, ** $P<0.01$, *** $P<0.001$.

also extends to wheat and that correct regulation of *Q* expression is required for normal formation of the wheat spike and spikelets.

MATERIALS AND METHODS

Plant materials and mutagenesis

The spring habit, bread wheat cultivar Sunstate (SS) was mutagenized using sodium azide as described by Chandler and Harding (2013). SS contains the domesticated *Q* allele. The same mutagenesis was performed on *Q'* grain

when generating revertant alleles. Further information regarding additional *Q* alleles, threshing and growth conditions is provided in the supplementary Materials and Methods.

Expression analysis by qRT-PCR

Developing inflorescence tissue was harvested for qRT-PCR at terminal spikelet stage. Five developing inflorescences were harvested per biological replicate. Peduncle internode tissue was harvested when the peduncle

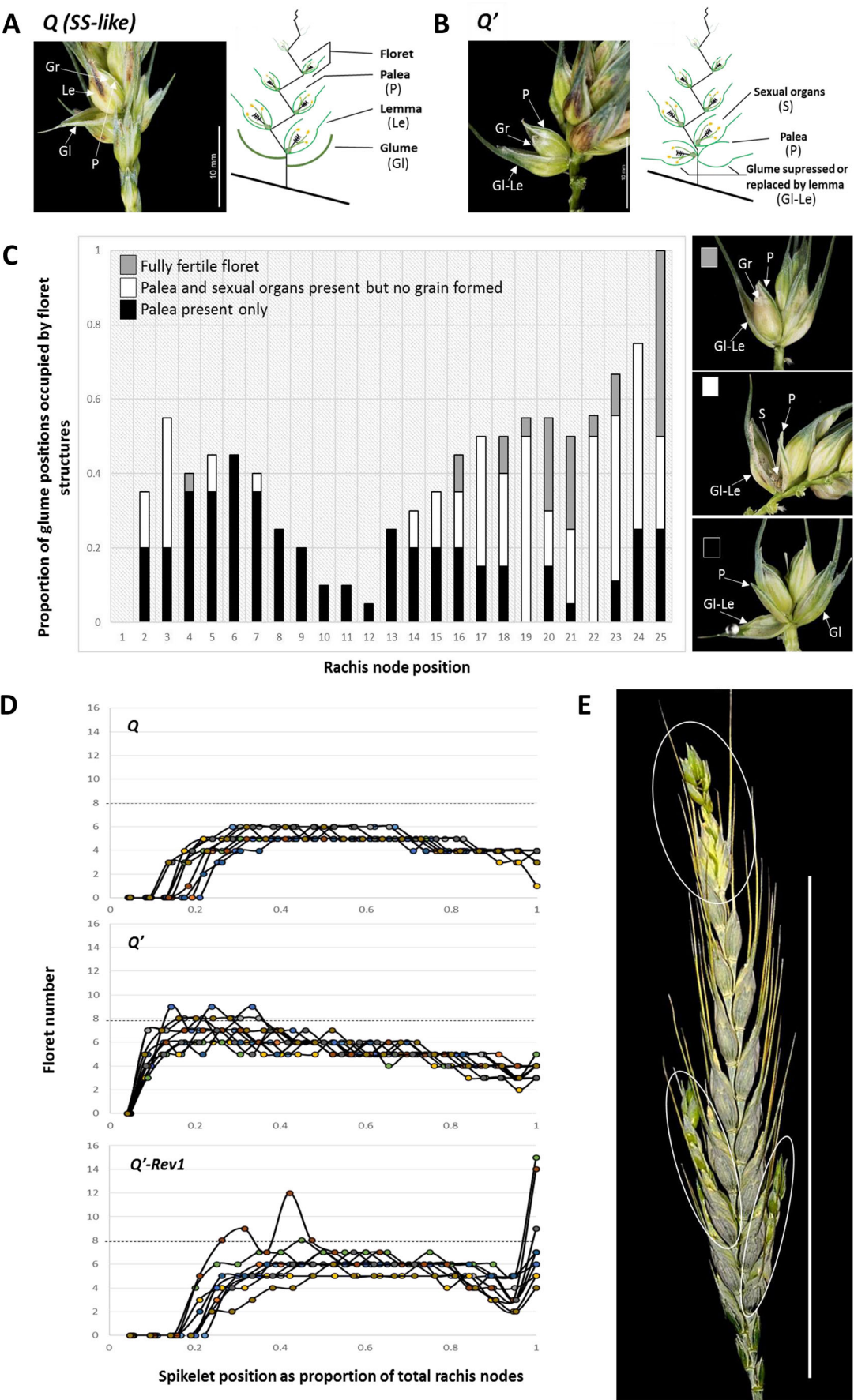


Fig. 4. See next page for legend.

Fig. 4. Detailed phenotyping of *Q*, *Q'* and *Q'-Rev1* plants reveals inflorescence architecture defects. (A) SS-like (*Q*) spikelet image and schematic showing typical wheat spikelet structure in which no ectopic florets form. (B) *Q'* spikelet, by contrast, shows a severe ectopic floret phenotype in which complete florets replace glumes. Scale bars: 10 mm in A,B. (C) *Q'* plants exhibit complete ectopic florets or floret-like structures in place of glumes, most frequently in the base and apical portions of the spike. Data are presented as the proportion of ectopic florets at each rachis node position across ten plants, where the total number of possible glumes is 2 per rachis node per plant. P, palea; Le, lemma; Gl, glume; Gr, grain; Gl-Le, glume-lemma; S, sexual organs. (D) Floret numbers of sequential spikelets from the base (left) to top (right) of spikes, where total spike length is set at 1 for *Q*, *Q'* and *Q'-Rev1* plants. Data are presented for each of ten individuals per genotype. Plot points mark individual spikelets (terminal spikelet at distance =1), with colors indicating separate spikes scored. Dotted line is for ease of comparison between genotypes. (E) *Q'-Rev1* spike illustrating elongated spikelets (sham ramification) containing many florets (circled). Scale bar: 10 cm.

internode of lines containing the *Q* domestication allele were 10 mm in length. A single peduncle internode was harvested for each biological replicate. Details of sample preparation and the qPCR protocol, including primers, are provided in the supplementary Materials and Methods and Table S1.

Modified 5' RACE

For 5' RACE, mRNA was purified from the same inflorescence RNA samples as used for the initial qRT-PCR analysis of *Q* in SS-like and *Q'* plants (Fig. 2). A GeneRacer Kit (Invitrogen) was used, except the de-capping protocol was not carried out, and the adapter was ligated directly to mRNA. Amplification of cleaved and ligated *Q* transcript was performed using gene-specific and GeneRacer adapter-specific primers (Table S1). Amplicon of the expected size was ligated into pGEM[®]-T Easy (Promega) before transformation, selection and sequencing of individual clones to determine cleavage location and frequency. See the supplementary Materials and Methods for more details.

Scanning electron microscopy (SEM)

Developing inflorescence samples were prepared for SEM with a Zeiss Evo LS15 scanning electron microscope as described in the supplementary Materials and Methods.

Sequence information

The miR172 sequence shown in this study is that of Ta-miR172a obtained from Yao et al. (2007). Although other isoforms have been reported and might contribute to regulation of *Q*, Ta-miR172a was used as a reference sequence for alignment purposes. *Q* sequence is available through GenBank accession AY702956.1.

Statistical analysis

Two-tailed Student's *t*-test was employed to compare means. Sample sizes (*n*) and *P*-values are given in figure legends.

Acknowledgements

We thank the ANU and CSIRO OCE PhD scheme for support to Julian Greenwood, Prof. John Evans for advice and supervision, Bjorg Sherman and Kerrie Ramm for technical help with mutant populations, and Carl Davies for photography.

Competing interests

The authors declare no competing or financial interests.

Author contributions

Conceptualization: J.R.G., E.J.F., B.T., S.M.S.; Methodology: J.R.G., E.J.F., B.T., S.M.S.; Validation: J.R.G., E.J.F.; Formal analysis: J.R.G., E.J.F.; Investigation: J.R.G., E.J.F.; Resources: J.R.G., N.W., B.T., S.M.S.; Writing - original draft: J.R.G., E.J.F., B.T., S.M.S.; Writing - review & editing: J.R.G., E.J.F., S.M.S.; Visualization: J.R.G.; Supervision: B.T., S.M.S.; Project administration: B.T., S.M.S.; Funding acquisition: S.M.S.

Funding

This work was supported by an Australian National University (ANU) University Research Scholarship and a Commonwealth Scientific and Industrial Research Organisation (CSIRO) OCE PhD Top-up Scholarship.

Supplementary information

Supplementary information available online at <http://dev.biologists.org/lookup/doi/10.1242/dev.146407.supplemental>

References

- Alieva, A. J. and Aminov, N. K. (2013). Influence of D genome of wheat on expression of novel type spike branching in hybrid populations of 171ACS line. *Russ. J. Genet.* **49**, 1119–1126.
- Amagai, Y., Aliyeva, A. J., Aminov, N. K., Martinek, P., Watanabe, N. and Kuboyama, T. (2014). Microsatellite mapping of the genes for sham ramification and extra glume in spikelets of tetraploid wheat. *Genet. Resour. Crop Evol.* **61**, 491–498.
- Amagai, Y., Aliyeva, A. J., Aminov, N. K., Martinek, P., Watanabe, N. and Kuboyama, T. (2015). Microsatellite mapping of the gene for sham ramification in spikelets derived from a hexaploid wheat (*Triticum* spp.) accession 171ACS. *Genet. Resour. Crop Evol.* **62**, 1079–1084.
- Aukerman, M. J. and Sakai, H. (2003). Regulation of flowering time and floral organ identity by a microRNA and its APETALA2-like target genes. *Plant Cell* **15**, 2730–2741.
- Boden, S. A., Cavanagh, C., Cullis, B. R., Ramm, K., Greenwood, J., Jean Finnegan, E., Trevaskis, B. and Swain, S. M. (2015). Ppd-1 is a key regulator of inflorescence architecture and paired spikelet development in wheat. *Nat. Plants* **1**, 14016.
- Brown, R. H. and Bregitzer, P. (2011). A Ds insertional mutant of a barley miR172 gene results in indeterminate spikelet development. *Crop Sci.* **51**, 1664.
- Chandler, P. M. and Harding, C. A. (2013). 'Overgrowth' mutants in barley and wheat: new alleles and phenotypes of the 'Green Revolution' Della gene. *J. Exp. Bot.* **64**, 1603–1613.
- Chuck, G., Meeley, R. B. and Hake, S. (1998). The control of maize spikelet meristem fate by the APETALA2-like gene indeterminate spikelet1. *Genes Dev.* **12**, 1145–1154.
- Chuck, G., Meeley, R., Irish, E., Sakai, H. and Hake, S. (2007). The maize tasselseed4 microRNA controls sex determination and meristem cell fate by targeting Tasselseed6/indeterminate spikelet1. *Nat. Genet.* **39**, 1517–1521.
- Chuck, G., Meeley, R. and Hake, S. (2008). Floral meristem initiation and meristem cell fate are regulated by the maize AP2 genes ids1 and sid1. *Development* **135**, 3013–3019.
- Debernardi, J. M., Lin, H., Chuck, G., Faris, J. D. and Dubcovsky, J. (2017). microRNA172 plays a crucial role in wheat spike morphogenesis and grain threshability. *Development* **144**, 1966–1975.
- Faris, J. D., Fellers, J. P., Brooks, S. A. and Gill, B. S. (2003). A bacterial artificial chromosome contig spanning the major domestication locus Q in wheat and identification of a candidate gene. *Genetics* **164**, 311–321.
- Förster, S., Schumann, E., Eberhard Weber, W. and Pillen, K. (2012). Discrimination of alleles and copy numbers at the Q locus in hexaploid wheat using quantitative pyrosequencing. *Euphytica* **186**, 207–218.
- Förster, S., Schumann, E., Baumann, M., Weber, W. E. and Pillen, K. (2013). Copy number variation of chromosome 5A and its association with Q gene expression, morphological aberrations, and agronomic performance of winter wheat cultivars. *Theor. Appl. Genet.* **126**, 3049–3063.
- Houston, K., McKim, S. M., Comadran, J., Bonar, N., Druka, I., Uzkre, N., Cirillo, E., Guzy-Wroblewska, J., Collins, N. C., Halpin, C. et al. (2013). Variation in the interaction between alleles of HvAPETALA2 and microRNA172 determines the density of grains on the barley inflorescence. *Proc. Natl. Acad. Sci. USA* **110**, 16675–16680.
- Jung, J.-H., Seo, Y.-H., Seo, P. J., Reyes, J. L., Yun, J., Chua, N.-H. and Park, C.-M. (2007). The GIGANTEA-regulated microRNA172 mediates photoperiodic flowering independent of CONSTANS in Arabidopsis. *Plant Cell* **19**, 2736–2748.
- Kosuge, K., Watanabe, N., Melnik, V. M., Laikova, L. I. and Goncharov, N. P. (2012). New sources of compact spike morphology determined by the genes on chromosome 5A in hexaploid wheat. *Genet. Resour. Crop Evol.* **59**, 1115–1124.
- Lauter, N., Kampani, A., Carlson, S., Goebel, M. and Moose, S. P. (2005). microRNA172 down-regulates glossy15 to promote vegetative phase change in maize. *Proc. Natl. Acad. Sci. USA* **102**, 9412–9417.
- Lee, D.-Y. and An, G. (2012). Two AP2 family genes, supernumerary bract (SNB) and Osindeterminate spikelet 1 (OsIDS1), synergistically control inflorescence architecture and floral meristem establishment in rice. *Plant J.* **69**, 445–461.
- Lee, D.-Y., Lee, J., Moon, S., Park, S. Y. and An, G. (2007). The rice heterochronic gene SUPERNUMERARY BRACKT regulates the transition from spikelet meristem to floral meristem. *Plant J.* **49**, 64–78.
- Mathieu, J., Yant, L. J., Mürdter, F., Küttner, F. and Schmid, M. (2009). Repression of flowering by the miR172 target SMZ. *PLoS Biol.* **7**, e1000148.
- Mlotshwa, S., Yang, Z., Kim, Y. and Chen, X. (2006). Floral patterning defects induced by Arabidopsis APETALA2 and microRNA172 expression in *Nicotiana benthamiana*. *Plant Mol. Biol.* **61**, 781–793.
- Schmid, M., Uhlenhaut, N. H., Godard, F., Demar, M., Bressan, R., Weigel, D. and Lohmann, J. U. (2003). Dissection of floral induction pathways using global expression analysis. *Development* **130**, 6001–6012.

- Simons, K. J., Fellers, J. P., Trick, H. N., Zhang, Z., Tai, Y.-S., Gill, B. S. and Faris, J. D.** (2006). Molecular characterization of the major wheat domestication gene Q. *Genetics* **172**, 547-555.
- Sormacheva, I., Golovnina, K., Vavilova, V., Kosuge, K., Watanabe, N., Blinov, A. and Goncharov, N. P.** (2015). Q gene variability in wheat species with different spike morphology. *Genet. Resour. Crop Evol.* **62**, 837-852.
- Varkonyi-Gasic, E., Lough, R. H., Moss, S. M. A., Wu, R. and Hellens, R. P.** (2012). Kiwifruit floral gene APETALA2 is alternatively spliced and accumulates in aberrant indeterminate flowers in the absence of miR172. *Plant Mol. Biol.* **78**, 417-429.
- Wang, L., Sun, S., Jin, J., Fu, D., Yang, X., Weng, X., Xu, C., Li, X., Xiao, J. and Zhang, Q.** (2015). Coordinated regulation of vegetative and reproductive branching in rice. *Proc. Natl. Acad. Sci. USA* **112**, 15504-15509.
- Yant, L., Mathieu, J., Dinh, T. T., Ott, F., Lanz, C., Wollmann, H., Chen, X. and Schmid, M.** (2010). Orchestration of the floral transition and floral development in Arabidopsis by the bifunctional transcription factor APETALA2. *Plant Cell* **22**, 2156-2170.
- Yao, Y., Guo, G., Ni, Z., Sunkar, R., Du, J., Zhu, J.-K. and Sun, Q.** (2007). Cloning and characterization of microRNAs from wheat (*Triticum aestivum* L.). *Genome Biol.* **8**, R96.
- Zhang, Z., Belcram, H., Gormicki, P., Charles, M., Just, J., Huneau, C., Magdelenat, G., Couloux, A., Samain, S., Gill, B. S. et al.** (2011). Duplication and partitioning in evolution and function of homoeologous Q loci governing domestication characters in polyploid wheat. *Proc. Natl. Acad. Sci. USA* **108**, 18737-18742.
- Zhu, Q.-H., Upadhyaya, N. M., Gubler, F. and Helliwell, C. A.** (2009). Over-expression of miR172 causes loss of spikelet determinacy and floral organ abnormalities in rice (*Oryza sativa*). *BMC Plant Biol.* **9**, 149.

Supplementary Materials and Methods

Plant material, threshing and growth conditions

Threshing was performed by hand and by the same person to gauge the threshability of mutant wheat lines. In reference to the loss-of-function mutant *Q'-Rev1* threshing required the identification of individual grain for removal by splitting apart florets and spikelets whereas in *Q'* and SS-like spikes, grain could easily be separated by rolling the spike back and forth between clapped palms.

The compact mutant near isogenic lines ANBW5B (5B D in Fig 3) and ANBW5C (5C D in Figure 3) were isolated and mapped by (Kosuge et al., 2011). The lines were established by backcrossing the mutants Cp-M808 (ANBW5B) and MCK 2617 (ANBW5C) with Novosibirskaya 67 (N67) for six generations. N67 contains the typical domesticated *Q* allele. The line 5C T included in Figure 3 represents an N67-like segregant from a line heterozygous for the ANBW5C mutation after backcrossing, however by this round of backcrossing N67 and N67-like segregants are effectively genetically identical.

Screening of mutant lines and phenotyping for co-segregation analysis was performed in glasshouse conditions with temperature controlled to ~22°C (Day) and ~16°C (Night) over Spring and Summer. All other phenotyping and tissue extraction for RNA was from plants grown in cabinets (Conviron PGC20) under 16h light (Measured at 420µM m⁻¹ s⁻¹ 50cm below light source) (22°C) and 8h dark (16°C).

Modified 5' RACE

mRNA was purified from the same inflorescence RNA samples used for the initial qRT-PCR analysis of *Q* in SS-like and *Q'* plants (Fig 2). A Gene-racer kit (Invitrogen) was used for 5'-RACE, except the de-capping protocol was not carried out, and the adapter was ligated directly to mRNA. Amplification of cleaved and ligated *Q* transcript was performed using gene specific and Gene-racer specific primers. Secondary nested PCR was performed to ensure amplification of gene specific products.

Amplification products were gel purified and ligated into pGEM®-T easy before being transformed into *E.coli* XL-Blue cells and selected on ampicillin plates containing 100 µL of 100mM IPTG and 20 µL of 50 mg/ml X-Gal. Individual colonies were selected and grown overnight in LB with 50 µg/ml ampicillin and purified using Qiagen mini-preps. In total, 96 colonies were selected for sequencing of *Q'* (n=48) and SS-like (n=48) amplification product. Only sequenced clones containing correct *Q* transcript sequence were included with the proportion of cleavage within the miR172-binding site presented. Gene specific primer sequences are listed in Supplementary Table 1.

qRT-PCR

All tissue was ground to fine powder in 1.5ml snap lock tubes containing two ball bearings using a mixermill. RNA extraction and DNase treatment was performed using the Maxwell® RSC Plant RNA Kit and Maxwell® RSC Instrument following the advised protocol. cDNA synthesis was performed using Maxima H-minus reverse transcriptase from invitrogen with oligo dT to prime mRNA using 5µg total RNA. cDNA was diluted 30 fold and 5µl of diluted cDNA was used in each qPCR reaction. qPCR was performed using SYBR Green on a Roche LightCycler®480II using RP15 as an endogenous control. Primers are shown in Supplementary Table S1.

Routine testing of cDNA samples was performed by serial dilution and calculation of R^2 from the standard curve. Analysis was performed using Roche LightCycler®480II and associated software. For all cDNA samples presented, 5 log serial dilutions were performed and R^2 values ≥ 0.982 were determined before qPCR analysis. Primer efficiency was calculated from the exponential phase of amplification in each reaction sample in each qRT-PCR run. qRT-PCR Primer pairs used in this study routinely achieved amplification efficiencies $\geq 90\%$.

Scanning Electron Microscopy (SEM)

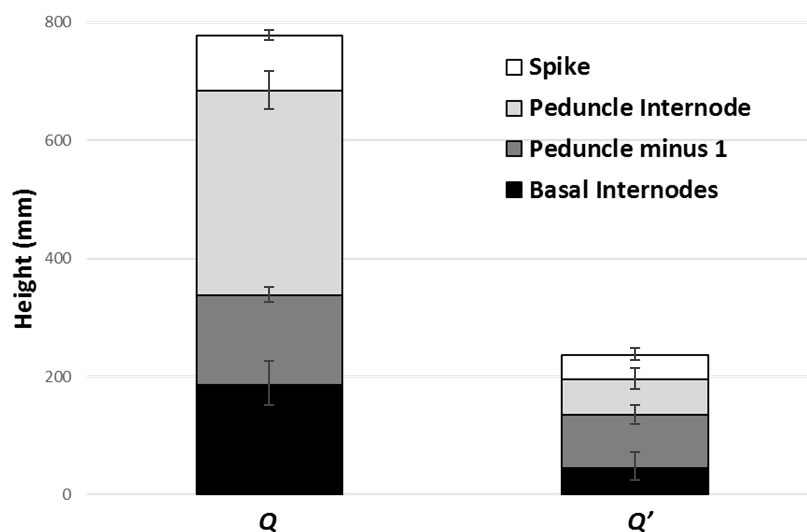
Developing inflorescence samples for SEM were prepared by immediate transfer to 100% ethanol after harvest. Ethanol was replaced twice daily until samples appeared completely white (2-3 days). Sample preparation adapted from (Talbot and White, 2013). Samples were then put through a critical point drying process in a tousimis autosamdri®-815 critical point drying device with purge timer set to 4. After critical point drying, samples were mounted on specimen stubs using adhesive carbon discs. Samples were imaged with a Zeiss Evo LS15 scanning electron microscope using backscattered electron detector (Gain= High), at 20KV and extended pressure setting (10pa).

Supplementary Table S1. Primers used in this study

Primer Name	Purpose	Sequence	
pJG31	<i>Q</i> Full genomic sequence	GATGGTGCTGGATCTCAATGTGG	
PJG33	<i>Q</i> Full genomic sequence	CAACAATGGCGGACTGCTG	
pJG14	<i>Q</i> genomic sequence spanning miRNA-Binding site	TCACTGCTGGTGCTGGTGC	
PJG18	<i>Q</i> genomic sequence spanning miRNA-Binding site	AAGTAGAACCGGTGGTGGTCC	
pJG38	Sequencing <i>Q</i>	CTACGAGGAGGATTTGAAGCAG	
pJG39	Sequencing <i>Q</i>	ACACGACACTCGATTGCAGAC	
pJG5	Sequencing <i>Q</i>	AATGAGGGTACTACTACAATCGGTC	
pJG2	Sequencing <i>Q</i>	CTACCCGAACGTACAGGTATCA	
pJG13	Sequencing <i>Q</i>	GGTGCAGGAGAGGCCCAT	
pJG29	<i>Q</i> specific 5' Race	GGAAGTAGAACCGGTGGTGGTCC	
pJG30	<i>Q</i> specific 5' Race Nested	GTGGTGGTCCGGGTACGGC	
<i>Q</i> qPCR F	<i>Q</i> qPCR	CCCTGAATCGTCAACCACAATG	(Simons et al., 2006)
<i>Q</i> qPCR R	<i>Q</i> qPCR	CCGTGCCATGTTGATGCA	(Simons et al., 2006)
TaRP15 F	Control gene qPCR	GCACACGTGCTTTGCAGATAAG	(Shaw et al., 2012)
TaRP15 R	Control gene qPCR	GCCCTCAAGCTCAACCATAACT	(Shaw et al., 2012)

miR172 Reverse transcription, expression, control primers associated methods used in this study can be found in companion paper Debernardi et al., 2017.

Supplementary Figures



Supplementary Figure 1 Internode elongation phenotype of Q' . Total height of Q' mutant and its sibling line containing the normal Q domestication allele with total height being shown as stacked histogram of average spike, peduncle internode, peduncle minus 1 and remaining basal internode lengths. $n=12$ plants. The number of basal peduncle internodes varied between two and three visible internodes amongst measured plants. The length of peduncle and peduncle internode were measured individually as differences in the length of these internodes, as well as the spike, accounted for most of the height reduction in Q' plants.

```

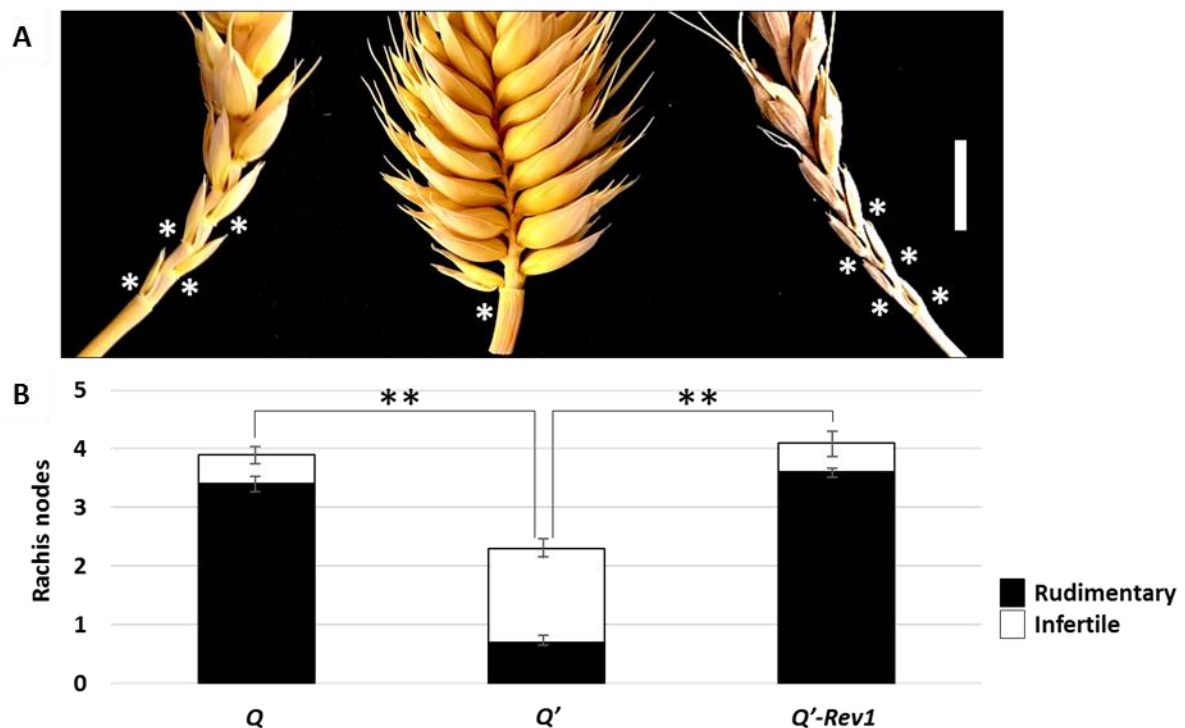
q  CTGCAGCATCATCAGGATTCT
Q  CTGCAGCATCATCAGGATTTT
Q' CTGCAGCATCATCAGAATTTT
Q'-like CTGCAACATCATCAGGATTTT
TaMIR172 UACGUCGUAGUAGUUCUAAGA

```

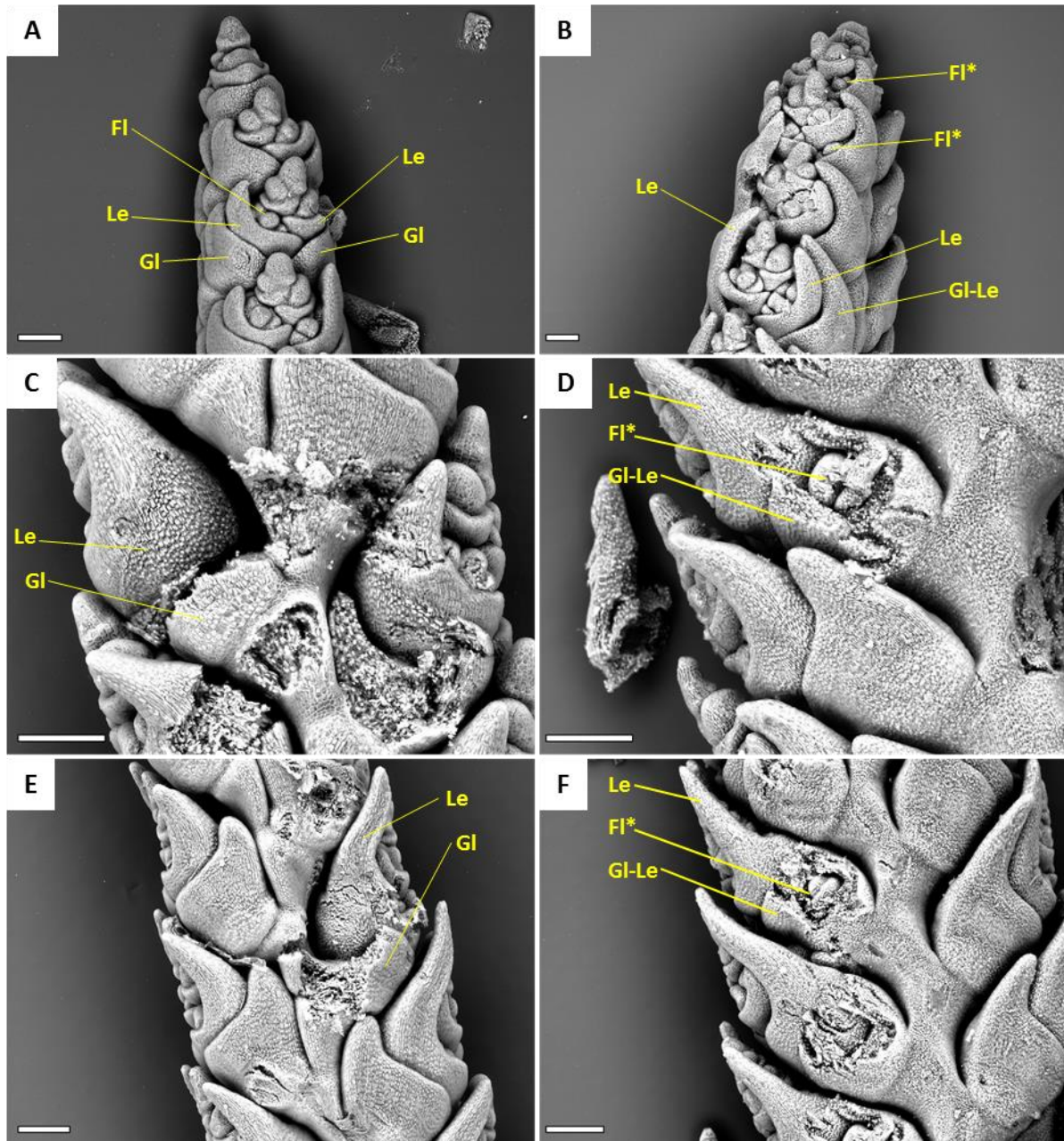
Supplementary Figure 2 miRNA-binding site alignments of pre-domesticated q , domesticated Q , gain-of-function alleles Q' and Q' -like. miRNA-binding site alignments and complementary *miRNA172* with mismatches shown in red and induced mismatches shown by red double underline.



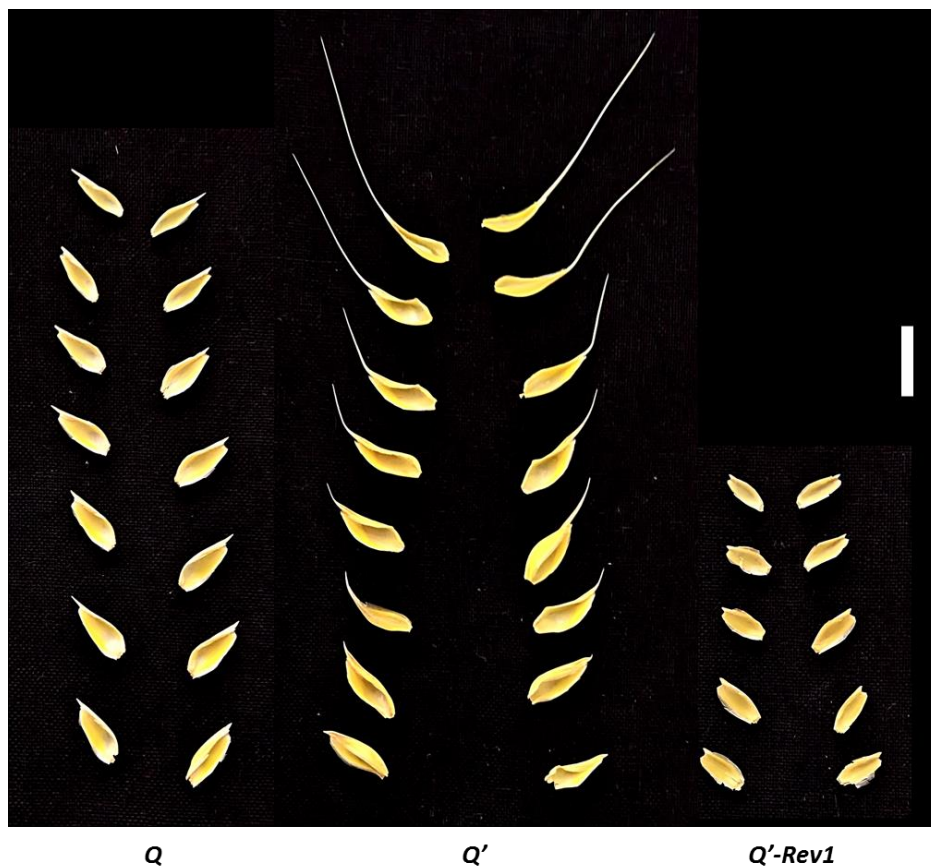
Supplementary Figure 3 The loss-of-function Q' -Rev1 is difficult to thresh A mechanical thresh test was performed by applying downward pressure to whole spikes with a hand threshing tool before sliding the tool horizontally. SS-like plants containing the domestication allele Q had spikes that were easy to thresh and Q' plants had spikes that were very easy to thresh with all grain separating from the head leaving an intact rachis. In contrast, Q' -Rev1 plants had spikes that were firm and required more pressure to thresh with some grain not separating from the spikelets. In addition, the rachis of Q' -Rev1 spikes had a greater tendency to break into individual nodes/spikelets. In each image the threshed rachis and intact spikelets have been arranged on the left hand side of the image. In Q and Q' plants, no grain remained bound in spikelets unlike Q' -Rev1.



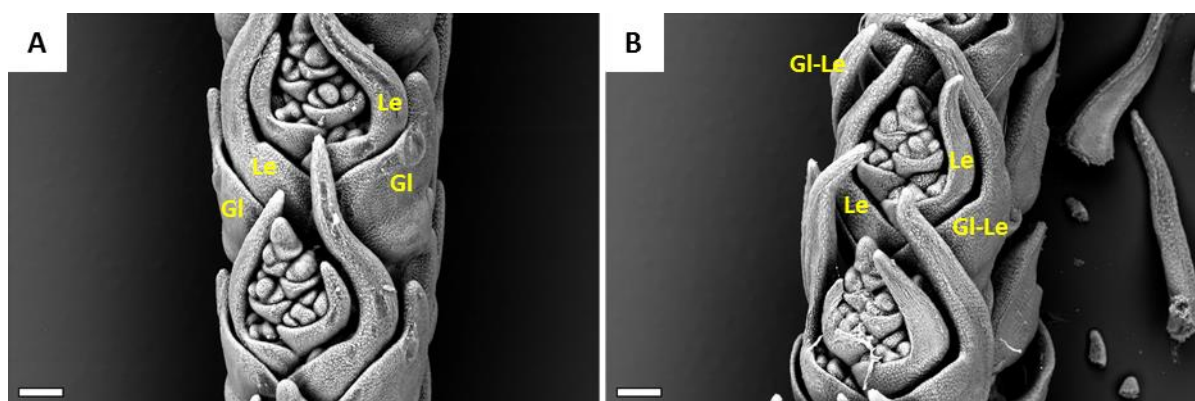
Supplementary Figure 4 The Q' mutant reduces the number of basal rudimentary (sterile) spikelets and produces fertile spikelets at basal rachis nodes that are unfilled in Q and the loss-of-function mutant Q' -Rev1. **A**, Basal portion of Q , Q' and Q' -Rev1 spikes. Rachis nodes with rudimentary spikelets (those lacking developed florets) are marked *. Scale bar=1cm. **B**, The average number of infertile spikelets (those that produced no grain) and the number of infertile spikelets which appeared to be rudimentary (without florets) in the basal portion of the main spike of Q , Q' and Q' -Rev1 plants. n=10. ** $P < 0.01$



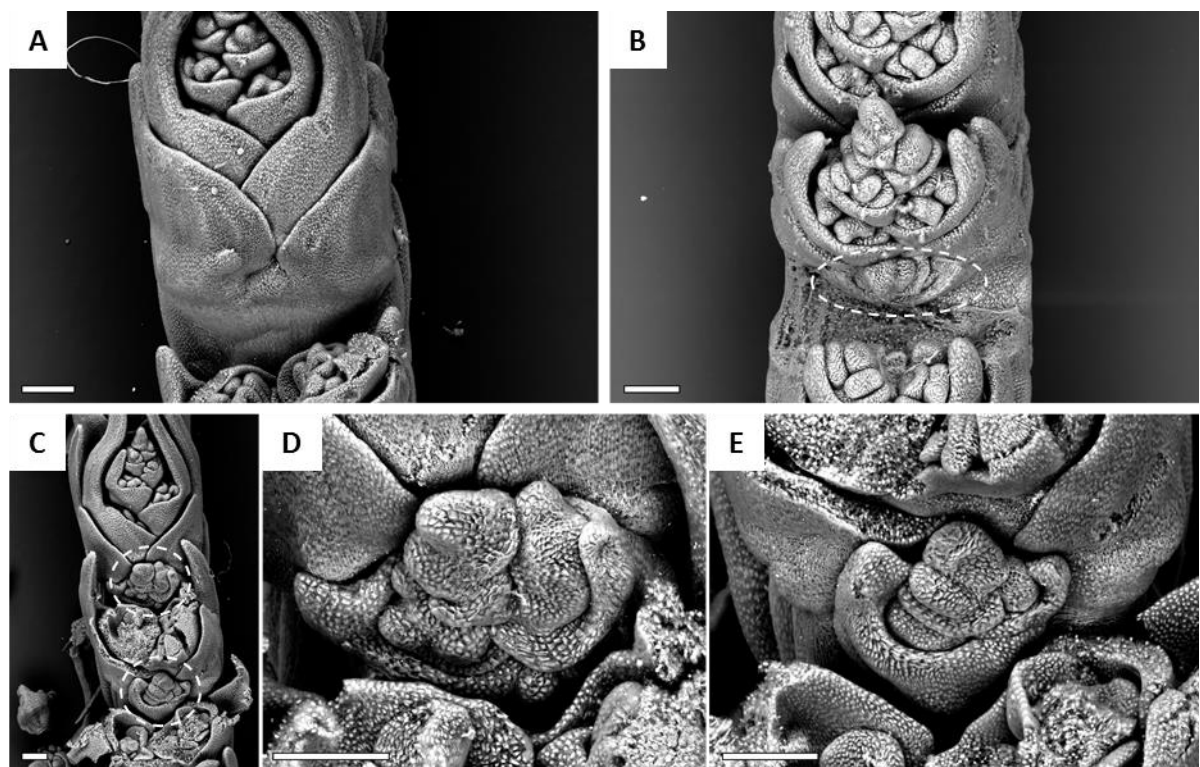
Supplementary Figure 5 Ectopic florets are produced in Q' spikelets. SEMs of *SS-like* (Left: A, C, E) and Q' (Right: B, D, F) spikes. Outer-most bracts have been removed from selected spikelets in C, D, E, F to reveal structures beneath. In the case of Q' ectopic florets (FI*) are visible beneath the outermost bracts of apical B, and dissected D, F, spikelets, while the outer-most bracts (glumes) of *SS-like* plants A, C, E feature typical sterile glumes. Scale bars= 200 μ m



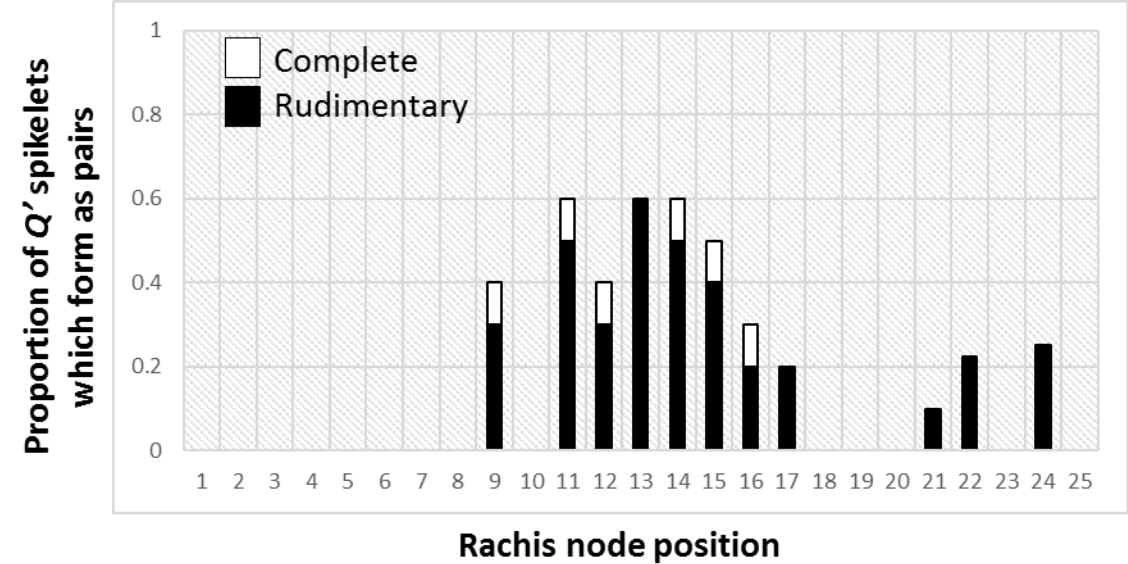
Supplementary Figure 6 Glumes of *Q'* mutant appear lemma-like with awns present in increasing length toward the apical portion of the spike. Glumes of *Q*, *Q'* and *Q'-Rev1* plants removed from one side of a single spike and placed in order to reflect their position on an intact and upright spike. Note that glumes of *Q'*, or the outermost positions on spikelets which should be occupied by glumes, are only similar to the glumes of *Q* when comparing basal spikelets. Scale bar= 1cm



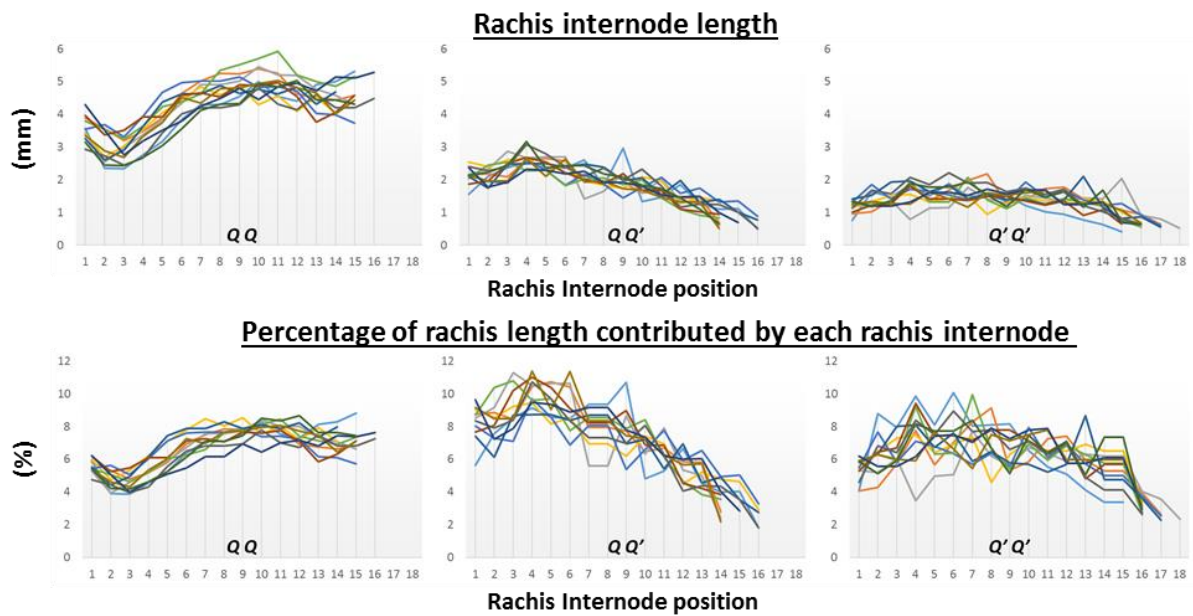
Supplementary Figure 7 Outer most bracts of *Q'* spikelets exhibit elongation of tips as in lemmas. SEMs of spikes shown are at comparable stages of inflorescence development when the tips of lemmas (awns) are beginning to elongate in both *SS*-like (*Q*) and *Q'* plants. The outermost bracts of *Q'* spikelets **B**, feature elongating tips much like a lemma at this stage whereas the outermost bracts of *Q* spikelets **A**, do not elongate and maintain short tips until maturity. See also **S Fig 5**. Gl= glume, Le= Lemma and Gl-Le= Glume-Lemma. Scale bars= 200µm



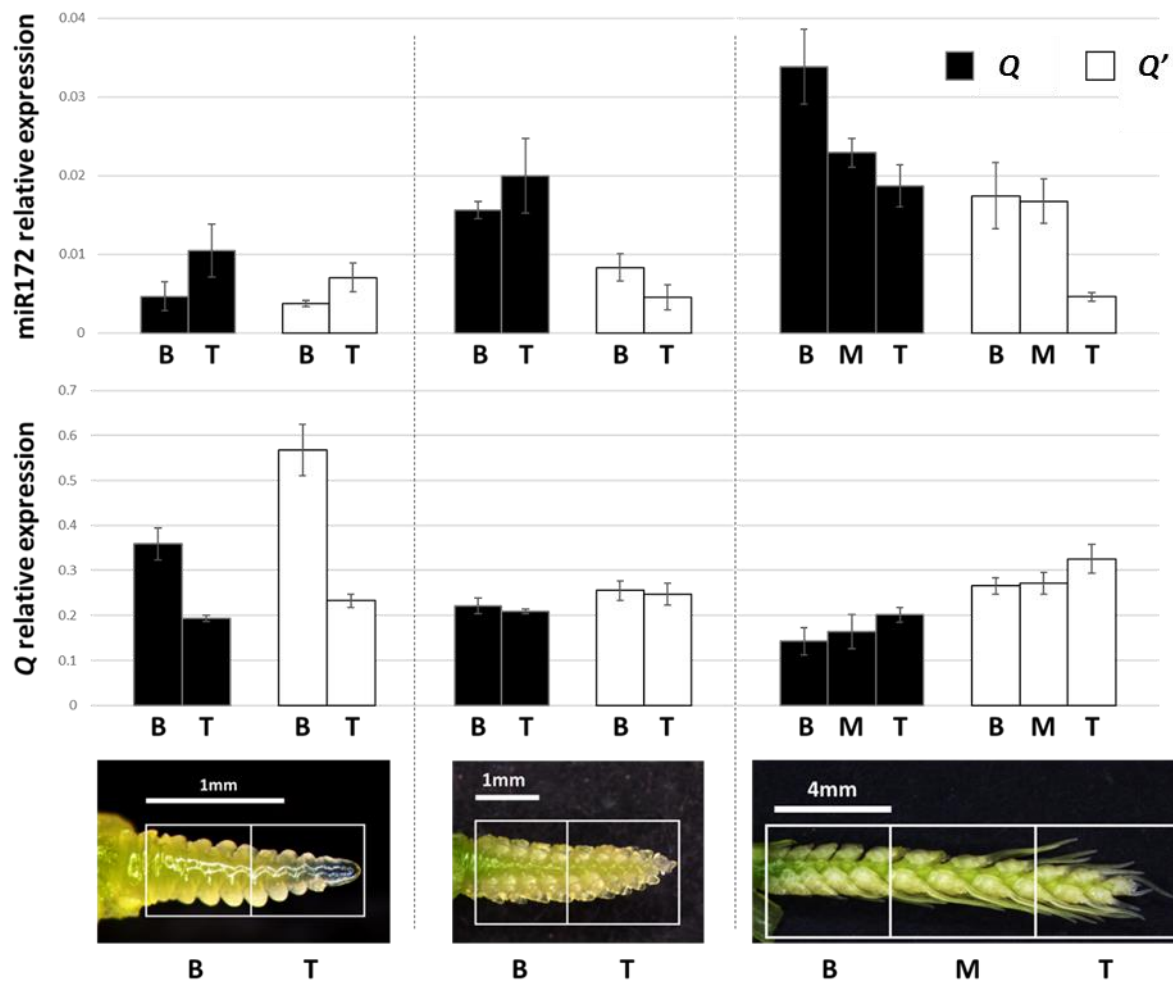
Supplementary Figure 8 Pairs of spikelets form at the central rachis nodes of *Q'* spikes. SEMs of dissected *SS*-like (*Q*) **A**, and *Q'* spikes **B**, **C**, **D**, **E**. to reveal the base of selected spikelets where spikelet pairs form, the spikelet beneath has been removed. The base of the *SS*-like spikelet shown in **A**, represents a typical single spikelet formation. The base of *Q'* spikelets in **B** and **D** show the formation of additional, or paired spikelet at the base of other spikelets. Scale bars= 200μm



Supplementary Figure 9 Proportion of paired spikelets in *Q'* plants forming at each rachis node. Paired spikelets at specific rachis node positions in *Q'* plants are shown as proportion of all spikelets scored at that rachis node position in main spikes of *Q'* plants. n= 10. Complete paired spikelets contained at least one macroscopic floret.



Supplementary Figure 10 Rachis internode elongation is reduced in plants containing the Q' with the most severe reduction in internode length occurring at the top of the spike. Rachis internode length profiles of SS-like ($Q Q$), heterozygous ($Q Q'$) and homozygous ($Q' Q'$) mutants where 1 equals the most basal rachis internode of the main spike. $n=12$. As rachis internode number varies between individuals, each individual has been plotted and represented by a different color.



Supplementary Figure 11 Spatial and temporal expression of Q and miR172. Images along the bottom of this figure correspond to the developmental stage at which spike sections were harvested. Expression analysis is shown relative to control genes for both Q and miR172. Data are presented as mean \pm s.e.m of 4 biological replicates in each section, at each timepoint.

Supplementary References

- Kosuge, K., Watanabe, N., Melnik, V. M., Laikova, L. I. & Goncharov, N. P. 2011. New sources of compact spike morphology determined by the genes on chromosome 5A in hexaploid wheat. *Genetic Resources and Crop Evolution*, **59**, 1115-1124.
- Shaw, L. M., Turner, A. S. & Laurie, D. A. 2012. The impact of photoperiod insensitive Ppd-1a mutations on the photoperiod pathway across the three genomes of hexaploid wheat (*Triticum aestivum*). *Plant Journal*, **71**, 71-84.
- Simons, K. J., Fellers, J. P., Trick, H. N., Zhang, Z., Tai, Y. S., Gill, B. S. & Faris, J. D. 2006. Molecular characterization of the major wheat domestication gene Q. *Genetics*, **172**, 547-555.
- Talbot, M. J. & White, R. G. 2013. Methanol fixation of plant tissue for Scanning Electron Microscopy improves preservation of tissue morphology and dimensions. *Plant Methods*, **9**, 36.